Nano Energy (2015) 13, 414–422

Available online at www.sciencedirect.com

ScienceDirect

journal homepage: www.elsevier.com/locate/nanoenergy

RAPID COMMUNICATION

Piezo-potential enhanced photocatalytic degradation of organic dye using ZnO nanowires

Xinyu Xue[a,b], Weili Zang[b], Ping Deng[b], Qi Wang[b], Lili Xing[b], Yan Zhang[a,c,*], Zhong Lin Wang[a,d,*]

[a]Beijing Institute of Nanoenergy and Nanosystems, Chinese Academy of Sciences, Beijing 100083, China
[b]College of Sciences, Northeastern University, Shenyang 110004, China
[c]Institute of Theoretical Physics, and Key Laboratory for Magnetism and Magnetic Materials of MOE, Lanzhou University, Lanzhou 730000, China
[d]School of Material Science and Engineering, Georgia Institute of Technology, Atlanta, GA 30332, USA

Received 20 January 2015; received in revised form 14 February 2015; accepted 17 February 2015
Available online 25 February 2015

KEYWORDS
Photocatalysis;
Piezoelectric;
ZnO nanowires;
Water pollution

Abstract
Piezoelectric semiconductors, such as wurtzite structure ZnO, GaN, and InN, have novel properties of coupling of piezoelectric and semiconductor. The piezoelectric field is created inside ZnO nanowires by applying strain. The photo-generated electrons and holes will be separated under the driving of piezoelectric field. The photocatalytic activity of ZnO nanowires for degrading methylene blue has been enhanced by the piezoelectric-driven separation of photo-generated carriers. Coupling the piezoelectric and photocatalytic properties of ZnO nanowires, a new fundamental mechanism for the degradation of organic dye has been demonstrated.

Introduction

Environmental pollution and energy shortage are among the most serious problems challenging the sustainable development of human civilization. As a major source of environmental pollution, water pollution caused by the waste discharged from organic chemicals in industry, fertilizer in agriculture and garbage of human living is an urgent issue to be addressed. Among various water treatment solutions, semiconductor photocatalysis using solar energy for purifying water sources is likely to be the most promising technologies because it is a green, energy-saving and facile way [1–6]. Recently, it has been demonstrated that their photocatalytic activity can be enhanced by the synthetic nanostructures [7–10]. For example, zinc oxide (ZnO) nanostructures have been intensively

*Corresponding authors.
E-mail addresses: zhangyan@lzu.edu.cn (Y. Zhang), zlwang@gatech.edu (Z.L. Wang).

http://dx.doi.org/10.1016/j.nanoen.2015.02.029
2211-2855/

investigated for water treatment due to their high photocatalytic efficiency, low cost and environmental friendliness [11-16]. Sunlight (UV) illumination on ZnO nanostructures induces a transition of electrons from the valence band to the conduction band, leaving an equal number of holes; then the photo-generated electrons and holes migrate to the surface accompanying reacting with absorbed electron donors and electron acceptors to form superoxide radical anions, hydrogen peroxides and hydroxyl radicals; finally the hydroxyl radicals can oxidize the organic compounds in aqueous solution, generating non-toxic CO_2 and H_2O. However, in this process a large proportion of photo-generated electron-hole pairs recombine before the photocatalysis takes place, dissipating the input solar energy and lowering down the photocatalytic efficiency. To prevent the recombination of electron-hole pairs, much effort has been made, such as developing novel nanostructures, loading co-catalysts (Pt, Pd and RuO_2), doping rare earth ions or transition metals, and introducing external electric field to yield an electrochemically assisted photocatalysis [11,15-21]. Although these methods have shown their potentials, high cost, complicate device structure and difficult operation restrain their practical applications at the industrial level.

Besides of semiconducting applications, ZnO nanowires for fabricating piezo-nanogenerators (NGs) have attracted world-wide attention due to their high piezoelectric output under applied deformation. And ZnO-based NGs have shown great performance in harvesting mechanical energy in the natural environment, such as wind, tide, sonic wave and atmospheric pressure [22-26]. When the *c*-axis of ZnO nanowire is under applied deformation, a piezoelectric field can be created on the surface. This piezoelectric field cannot only drive the electrons in the external circuit flowing forward and back, but also make the carriers inside ZnO nanowires migrate and partially screen this piezoelectric field. In this case, electrons and holes in ZnO nanowires migrate on the opposite directions as a separation of carriers. If the piezoelectric properties and the photocatalytic characteristics of ZnO nanowires can be coupled into a single internal physical-chemical process, then their photocatalytic efficiency could probably be enhanced by the piezo-driven separation of photo-generated electron-hole pairs.

In this paper, we establish a new fundamental piezo-photocatalytic mechanism that can co-use the photonic and mechanical energy for the degradation of organic dye by coupling the piezoelectric and photocatalytic properties of ZnO nanowires. The photocatalytic activity of ZnO nanowires for degrading methylene blue (MB) has been enhanced by the piezo-driven separation of photo-generated electron-hole pairs. Under UV irradiation and applying deformation on ZnO nanowires, the photo-generated electrons and holes migrate to the surface under the driving of piezoelectric field on the opposite directions, in which the electron-hole recombination can be suppressed. Compared with non-piezo-assisted photocatalyitic process, the more surface holes in the internal piezo-photocatalytic process can form more hydroxyl radicals to oxidize more organic compounds, resulting in higher photocatalytic efficiency. Such a new water-pollution treatment will be an important development of green technologies for the environment improvement.

Results and discussion

The experimental design proposed for our study is shown in Figure 1. ZnO nanowires are vertically aligned on carbon fibers (CFs) by a simple seed-assisted hydrothermal method,

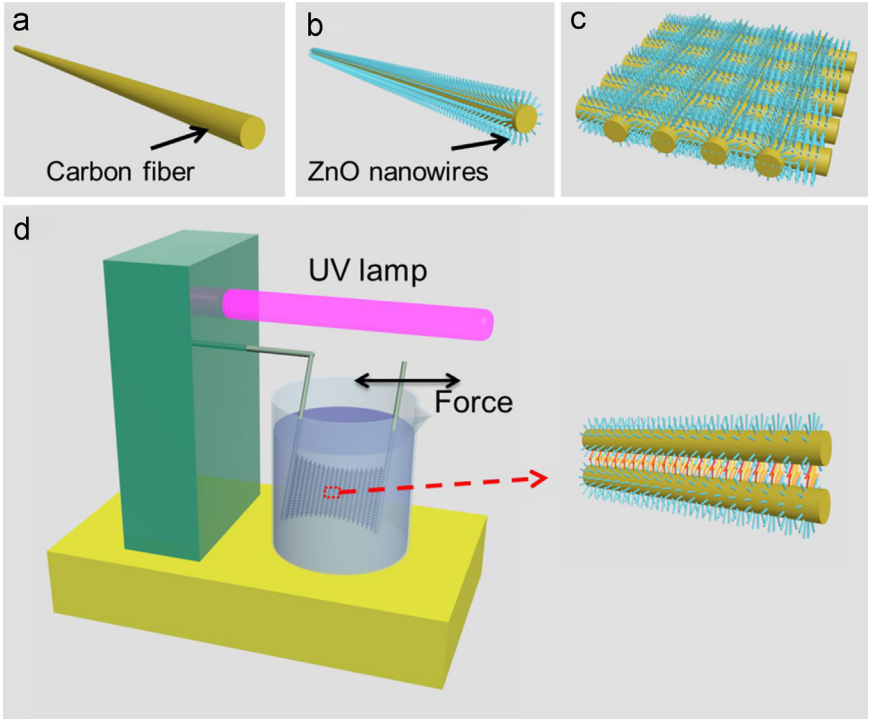

Figure 1 Experimental design proposed for our study. (a-c) Schematic images showing the fabrication process of the woven ZnO nanowires/CFs. (d) The degradation of MB solution by the piezo-photocatalytic activity of ZnO nanowires/CFs under UV irradiation and periodically applied force. The inset is the piezo-photocatalytic process in ZnO nanowires/CFs.

as shown in Figure 1a and b. ZnO nanowires are vertically aligned on the CF along the ZnO seed layer. It should be noted that the ZnO seed layer coating on the CFs is of polycrystalline structure and can serve as a buffer layer with low electric conductance to avoid short circuit state of ZnO nanowires. Several bundles of ZnO nanowires/CFs are then woven together, as shown in Figure 1c. The final device was made of multi-fibers. The degradation of MB by the piezo-photocatalytic activity of ZnO nanowires/CFs is performed in an aqueous solution under UV irradiation and periodically applied force, as shown in Figure 1d. When the ZnO nanowires/CFs are under mechanically brushing/sliding by the externally applied force (the inset of Figure 1d), ZnO nanowires extrude outward radially and they are against each other when the CFs are aligned. A mechanical pulling of one of the CF results in the bending of ZnO nanowires that produces a piezoelectric field across their width. This piezoelectric field drives photo-generated electrons and holes migrating to the surfaces on opposite directions, which could reduce the recombination of holes and electrons, and enhance the photocatalytic efficiency of ZnO nanowires.

The working mechanism for the piezo-photocatalytic activity of ZnO nanowires is shown in Figure 2. The woven ZnO nanowires/CFs are immersed into the MB aqueous solution, as schematically shown in Figure 2a. When ZnO nanowires are under UV light irradiation, the electrons in the valence band are excited to the conduction band, leaving an equal number of holes in the valence band (Figure 2b). As a periodic force is applied on ZnO nanowires/CFs, there is a relative sliding between the neighboring ZnO nanowires, leading to the bending of ZnO nanowires. As shown in Figure 2c, a piezoelectric field can be created across its width with negative piezo-potential on the compressive strain region (red) and positive piezo-potential on the tensile strain region (yellow), driving the photo-generated electrons migrating to the positive piezo-potential surface and the holes to the negative piezo-potential surface. Thus this piezo-driven carrier migration reduces the recombination rate of photo-generated electrons and holes, and more carriers can migrate to the surface. Then photo-generated holes at the negative surface react with hydroxyl groups to produce free •OH radicals, and the photo-generated electrons at the positive surface react with O_2 to produce $\bullet O_2^-$ groups (Figure 2d). The free hydroxyl radicals can oxidize MB in aqueous solution, generating non-toxic CO_2 and H_2O [27-29]. The physical-chemical reactions in this piezo-photocatalytic process are as follows:

$$\text{ZnO nanowires} + h\nu \overset{\text{piezoelectric field}}{\Longrightarrow} e^-(\text{positive surface}) + h^+(\text{negative surface}) \quad (1)$$

$$e^- + O_2 \rightarrow \bullet O_2^- \quad (2)$$

$$h^+ + OH^- \rightarrow \bullet OH \quad (3)$$

$$\bullet OH + MB \rightarrow CO_2 + H_2O \quad (4)$$

Compared with non-piezo-assisted photocatalyitic process, the more holes at the surface in this internal piezo-photocatalytic process can form more hydroxyl radicals to oxidize more organic compounds, resulting in higher photocatalytic efficiency. It should be pointed that in liquid environment, the piezo-potential created by ZnO nanowires not only drives the internal charges, but also drives free ions towards its surface to compensate the piezo-charge, [30] and the effective potential for the piezo-photocatalytic process is not as high as the output of the outside solid-state nanogenerator. Such a new piezo-photocatalytic mechanism can be applied by not only piezoelectric nanowires, but also nano-film and even bulk piezoelectric semiconductors.

Figure 3a and b shows typical SEM images of ZnO nanowires/CFs, showing that ZnO nanowire arrays are vertically aligned on the surface of CFs. The average diameter and length of ZnO nanowires are 500 nm and 6 μm, respectively. Figure 3c is a high resolution TEM image of the tip region of ZnO nanowire, showing that the lattice fringe spacing is 0.52 nm, corresponding to (0001) plane of ZnO crystal. The growth direction of ZnO nanowire is along the *c*-axis. Figure 3d is the X-ray diffraction (XRD) patterns of ZnO nanowires/CFs and bare CFs. The broad peak centered around 25° arises from the (002) plane of the carbon structures in CFs. The sharp diffraction peaks in curve 1 can be perfectly indexed to the hexagonal wurtzite structure of ZnO crystals (JCPDS 36-1451). No other peaks for impurity can be observed, suggesting that the composition of the samples is ZnO and carbon.

According to the method reported previously, [31] the multi-fiber NGs have been fabricated and measured. One single yarn woven from ~40 fibers is tested; ~20 fibers are Au-coated ZnO nanowires/CFs and the other ~20 fibers are non-Au-coated ZnO nanowires/CFs. The Au-coated ZnO nanowires/CFs are movable in the testing, and the non-Au-coated fibers are fixed. The Au-coated and non-Au-coated fibers are electrically connected to the external measurement circuit as the NG electrodes, respectively. When a pulling force is applied on the Au-coated fibers by a stepper motor, the Au-coated and non-Au-coated fibers have a relative sliding movement and a brushing movement can be achieved between the non-Au-coated nanowires and Au-coated nanowires. The experimental vibration on the woven yarn (~10 cm) is about 1 cm. Figure 4 demonstrates the piezoelectric effect of ZnO nanowires/CFs upon applied deformation. The short-circuit current is about 0.5 nA, and the open-circuit voltage is about 20 mV. Based on the mechanism of fiber nanogenerator in Ref. [31], a piezoelectric field in the non-Au-coated ZnO nanowire can be created across its width due to the deformation with negative piezo-potential on the compressive strain region and positive piezo-potential on the tensile strain region. The Au-coated nanowires act as the electrode for collecting and transporting the charges through Au/ZnO interface. The piezo-potential of ZnO nanowires and Schottky barrier of Au/ZnO lead to the DC piezoelectric output.

The piezo-photocatalytic activity of ZnO nanowires for degrading MB solution is shown in Figure 5. Figure 5a and b shows UV-vis absorption spectra of MB solution (C_0=5 mg/L, C_0 is initial concentration) upon photodegradation catalyzed by ZnO nanowires/CFs (200 mg) at different UV irradiative times with and without piezo-assistance, respectively. The spectra range from 350 to 700 nm with a peak at the wavelength of ~660 nm. It can be seen that the intensity of the absorption peak decreases with increasing degradation time. And the piezo-assistance can significantly enhance the photocatalytic activity of ZnO nanowires. With piezo-assistance (in Figure 5a, the periodically applied force is 1 Hz, and the woven CFs is under ~1 cm of vibration), after 120 min of UV irradiation, the degradation of MB solution is

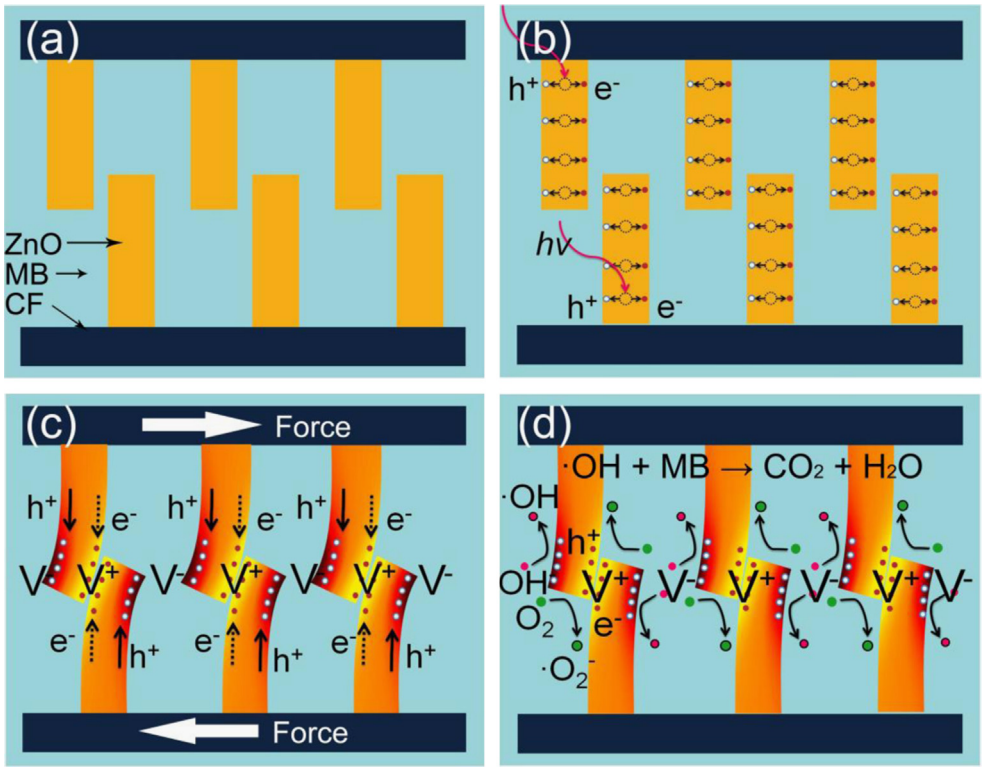

Figure 2 The working mechanism for the piezo-photocatalytic activity of ZnO nanowires. (a) Schematic illustration of the woven ZnO nanowires/CFs without applied force and UV irradiation. (b) When the UV light is on, UV illumination on ZnO nanowires induces a transition of electrons from the valence band to the conduction band, leaving an equal number of holes. (c) When the periodic force is applied on ZnO nanowires/CFs, there is a relative sliding between neighboring ZnO nanowires, resulting in the bending of ZnO nanowires which produces positive and negative piezoelectric potentials across their width. And the piezoelectric field drives the electrons and holes migrating to the surface in opposite directions. The recombination of electrons and holes can be reduced. (d) The electrons (e^-) react with dissolved oxygen molecules to yield superoxide radical anions ($\bullet O_2^-$), and the holes (h^+) are ultimately trapped by hydroxyl groups (or H_2O) at the surface to yield $\bullet$OH radicals. The hydroxyl radicals can oxidize MB in aqueous solution, generating non-toxic CO_2 and H_2O. The photocatalytic efficiency of ZnO nanowires is enhanced by the piezo-assistance due to the reduced recombination of photo-generated carriers.

up to 96%. In contrast, the degradation of MB solution without piezo-assistance (Figure 5b) is merely 64% after 120 min. The insets of Figure 5a and b display the decoloration of MB solution at different times with and without piezo-assitance, respectively. The piezoelectric potential is created when the ZnO nanowire is under applied external strain. As a result, the photo-generated electron-hole pairs will be separated by the piezoelectric potential. The piezo-potential prevents the recombination of electron-hole pairs inside the ZnO nanowire and increases the electrons and holes at different surfaces of ZnO nanowire. Therefore, the electron-hole pair separation effect by the piezo-potential will increase the photocatalytic efficiency of ZnO nanowires.

Photodegradation profiles of MB solution catalyzed by ZnO nanowires/CFs are shown in Figure 5c, and the applied force is under different frequencies: 1 Hz, 0.5 Hz and 0 (representing non-piezo-assistance). It can be seen that the photocatalytic activity of ZnO nanowires/CFs increases with increasing frequency of applied force simply due to higher input power. Kinetic curves of MB degradation catalyzed by ZnO nanowires/CFs are shown in Figure 5d. Without piezo-assistance (frequency=0), the linearity of the curve is similar to various reports on the photocatalytic properties of ZnO nanostructures, indicating that the kinetics for the photocatalytic decomposition of MB solution without applied force follows a pseudo first order rate [27,32]. Interestingly, with piezo-assistance, nonlinear curves can be observed, and the rate increases with time. It should also be noted that future work needs to be done to further improve the piezo-photocatalytic performance, such as synthesizing new composite materials and designing new device structures.

One of the important issues in photocatalyst is reproducibility, and the cycling performance of the piezo-photocatalytic activity of ZnO nanowires for degrading MB solution (the force frequency is 1 Hz) is shown in Figure 5e. At the first, second and third cycle, the degradation of MB solution after 120 min is about 98.8%, 99.4% and 98.8%, respectively. This result exhibits high reproducibility.

As shown in Figure 5f, the dye degradation under mechanical vibration only (without UV) has been tested. It can be seen that the dye concentration keeps stable under this condition. This result confirms that the dye degradation comes from the photocatalytic effect of the ZnO and the piezoelectric effect of ZnO cannot generate extra carriers. The piezoelectric effect of ZnO plays a supporting role in the piezo-photocatalytic process of ZnO nanowires for degrading MB solution.

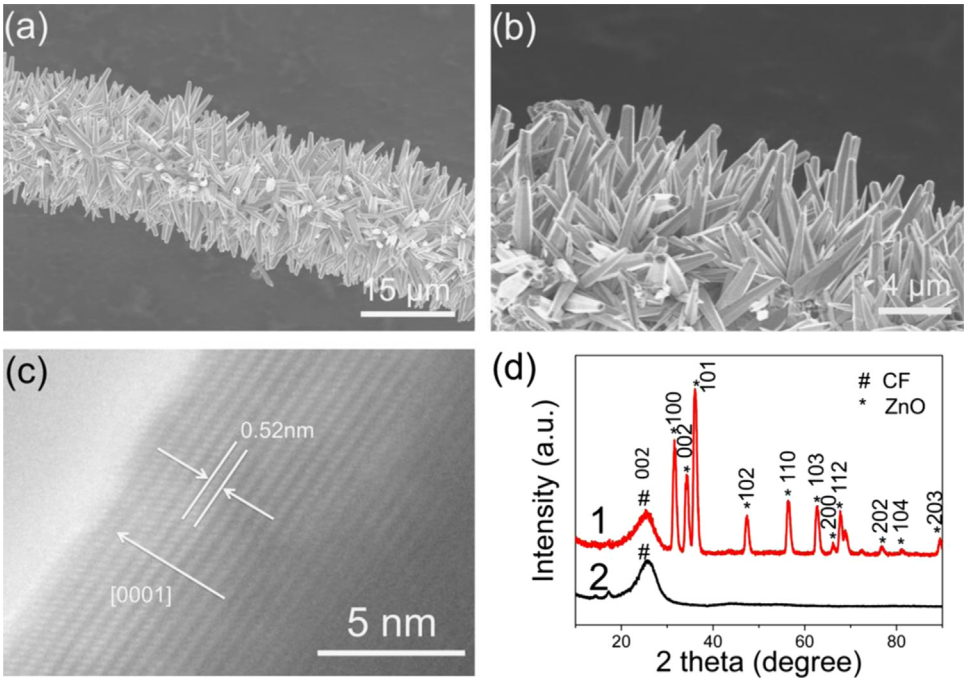

Figure 3 (a, b) SEM images of ZnO nanowires/CFs. (c) high resolution TEM image of the tip region of ZnO nanowire. (d) XRD patterns of ZnO nanowires/CFs (curve 1) and bare CFs (curve 2).

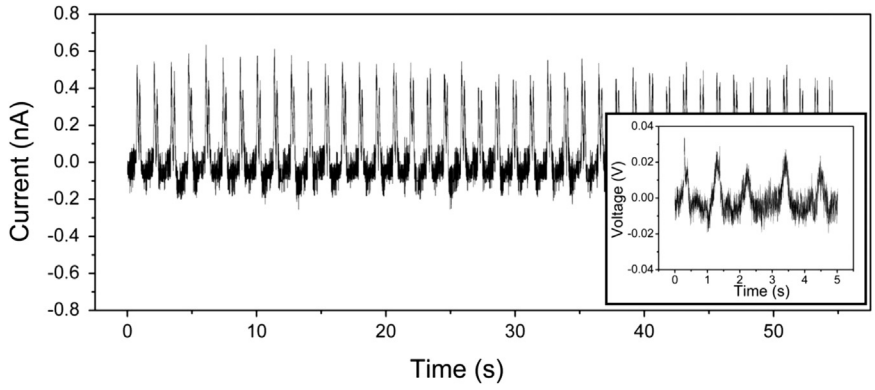

Figure 4 The piezoelectric output of the NG based on ZnO nanowires/CFs and Au-coated ZnO nanowires/CFs under a periodic pulling force, show the successful creation of piezoelectric potential in the nanowires.

As comparison experiments, piezo-photocatalytic degradation of MB solution is carried out by using ZnO nanoparticle/CFs, vertically-aligned ZnO nanowires on ITO (Indium tin oxide) glass and randomly-distributed ZnO nanowires on ITO glass, respectively, as presented in Supporting information. Figure S1 shows the photocatalytic degradation of MB solution by using ZnO nanoparticle/CFs with and without applying force, respectively. It can be seen that there is no obvious enhancement of photocatalytic activity of ZnO nanoparticles/CFs with applying force. The slopes of the kinetic curves of MB degradation catalyzed by ZnO nanoparticle/CFs with and without applying force are almost the same. The large amounts of ZnO nanoparticles have no uniform *c*-axis direction, which is similar to the polycrystalline structure. And the zero-dimensional structures of ZnO nanoparticles have very limited deformation on *c*-axis upon sliding (they cannot be bended), resulting in almost no piezoelectric output [33,34]. The recombination of electron-hole pairs cannot be prevented. This result confirms that the enhancement of photocatalytic efficiency of ZnO nanowires/CFs arises from the piezo-assistance. Figure S2 shows the photocatalytic degradation of MB solution by using vertically-aligned ZnO nanowires on ITO glass with and without applying compressive force, respectively. It can be seen that the photocatalytic activity of vertically-aligned ZnO nanowires on ITO glass is enhanced by the compressive force. The vertically-aligned ZnO nanowires have uniform *c*-axis direction, and under applied compressive force, the deformation on the *c*-axis can generate piezoelectric output. The recombination of electron-hole pairs can be prevented. This result further confirms that the enhancement of photocatalytic efficiency of ZnO nanowires arises from the piezo-assistance. Figure S3 shows the photocatalytic degradation of MB solution by using randomly-distributed ZnO nanowires on ITO glass with and without applying compressive force, respectively. It can be seen that there is a very small enhancement of

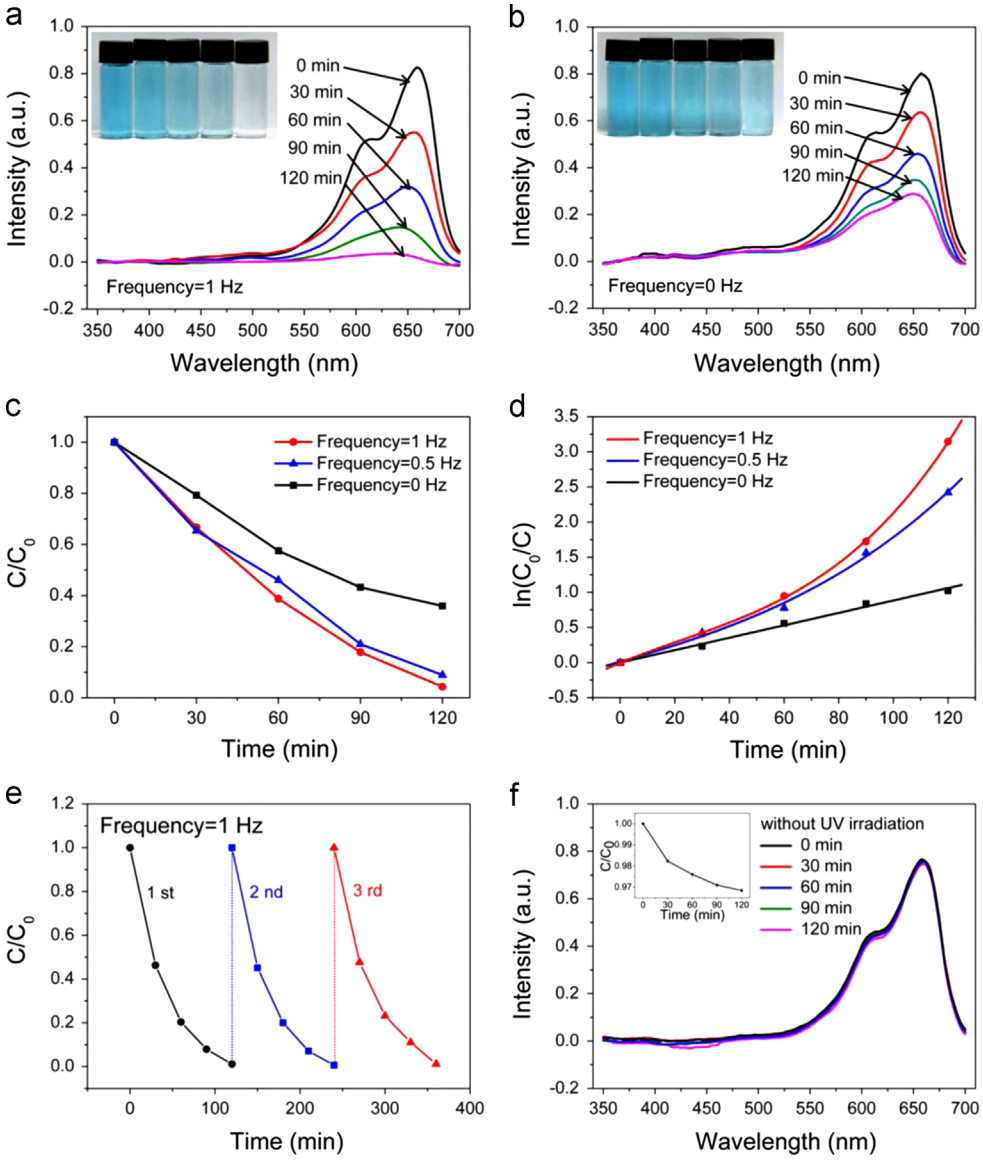

Figure 5 Piezo-photocatalytic activity of ZnO nanowires for degrading MB solution. (a, b) UV-vis absorption spectra of MB solution upon photodegradation catalyzed by ZnO nanowires/CFs at different UV irradiative times with piezo-assistance (the periodically applied force is 1 Hz, and the woven CFs is under ~1 cm of vibration) and without piezo-assistance (no force is applied), respectively. The insets are photographs of MB solutions upon degradation at different times. (c, d) Photodegradation profiles and kinetic curves of MB solution catalyzed by ZnO nanowires/CFs, respectively. The applied force is at different frequencies, and "Frequency=0" represents non-piezo-assisted photocatalytic process. (e) The cycling performance of the piezo-photocatalytic activity of ZnO nanowires for degrading MB solution (the force frequency is 1 Hz). Each cycle is 120 min. (f) The dye degradation under mechanical vibration only (without UV).

photocatalytic activity of randomly-distributed ZnO nanowires with applying compressive force. The randomly-distributed ZnO nanowires have no uniform *c*-axis direction, and have limited deformation on *c*-axis under compressive force (the force is vertical to the *c*-axis of most ZnO nanowires), resulting in weak piezoelectric output. The recombination of electron-hole pairs can hardly be prevented. This result further confirms that the enhancement of photocatalytic efficiency of ZnO nanowires arises from the piezo-assistance.

The piezoelectric potential distribution along ZnO nanowires is calculated by using finite element method (FEM), as shown in Figure 6a. The length and diameter of ZnO nanowire are l=6 μm and d=500 nm, respectively. According to previous theoretical works, [35,36] the applied stress is chosen as 40 MPa. The material constants used in the calculation are: elastic constants c11=207 GPa, c12=117.7 GPa, c13=106.1 GPa, c13=106.1 GPa, c33=209.5 GPa, c44=44.8 GPa, and c55=44.6 GPa, piezoelectric constants e15=−0.45 C/m^2, e31=−0.51 C/m^2, and e33=1.22 C/m^2. The relative dielectric constants are $\kappa^r_{\perp}=7.77$ and $\kappa^r_{//}=8.91$. Figure 6a shows the distribution of piezo-potential in the nanowire at its side cross-section parallel to its *c*-axis. The maximum value of piezo-potential increases linearly with the external stress, as shown in Figure 6b.

Under applied the piezoelectric field, the charge carriers will drift in a piezoelectric semiconductor. The positive

piezoelectric charges attract the electrons and the negative piezoelectric charges holes, resulting the photo-generated electron and hole separations and transports. According to semiconductor physics, the basic equations describing the dynamic carrier transport behavior in semiconductors is current-density equations and continuity equations [37]. The current-density equations are as follows:

$$\begin{cases} J_n = q\mu_n nE + qD_n\nabla n \\ J_p = q\mu_p pE - qD_p\nabla p \\ J_{cond} = J_n + J_p \end{cases} \quad (5)$$

where J_n and J_p are the electron and hole current density, μ_n and μ_p are electron and hole mobility, n and p are concentrations of free electrons and free holes, D_n and D_p are diffusion coefficients for electrons and holes, respectively, q is the absolute value of unit electronic charge, E is electric field, and J_{cond} is the total current density. The continuity equations are as follows:

$$\begin{cases} \frac{\partial n}{\partial t} = G_n - U_n + \frac{1}{q}\nabla J_n \\ \frac{\partial p}{\partial t} = G_p - U_p - \frac{1}{q}\nabla J_p \end{cases} \quad (6)$$

where G_n and G_p are the electron and hole generation rates, U_n and U_p are the recombination rates, respectively.

In a single nanowire under applied external strain, the deformation of ZnO nanowires increases gradually and the piezoelectric field increases gradually. The carriers will redistribute when the piezoelectric field is generated in ZnO nanowire. According to piezotronic theory, the current-density equations and continuity equations can be solved by numerical simulation for understanding the photo-generated electron-hole pair separation under piezoelectric potential [38]. For example, the photo-generated electron and hole concentration are chosen as $n_0=2.5\times10^{17}\ cm^{-3}$ and $p_0=2.5\times10^{17}\ cm^{-3}$ at thermal equilibrium. Figure 6c shows the distribution of electron concentrations under positive piezo-potential in the nanowire at its cross-sectional diameter parallel to y-axis, apparently displaying the effect of piezoelectric charges on the electron distribution. The electron concentration increases under positive piezo-potential, which shows a maximum value at left side of the ZnO nanowire, where the local positive piezoelectric charges accumulate. Alternatively, the negative piezoelectric charges attract the holes, resulting in a maximum value at right side of the ZnO nanowire, as shown in Figure 6d. Therefore, the photo-generated electron-hole pairs are separated by piezoelectric potential. With piezoelectric field, the hole concentration at right-hand side increases, resulting in the more holes which can react with more hydroxyl groups to produce more ●OH free radicals.

Conclusion

In summary, a new fundamental piezo-photocatalytic mechanism that couples the piezoelectric and photocatalytic properties of ZnO nanowires was demonstrated. The photocatalytic activity of ZnO nanowires for the degradation of MB solution was enhanced by the piezo-driven separation of photo-generated electron-hole pairs. Under UV illumination and applying deformation on ZnO nanowires, the photo-generated electrons and holes migrated to the surfaces under the driving of piezoelectric field on the opposite directions, in which the electron-hole recombination could be supressed. Such a new piezo-photcatalytic process could be extended to the co-utilization of

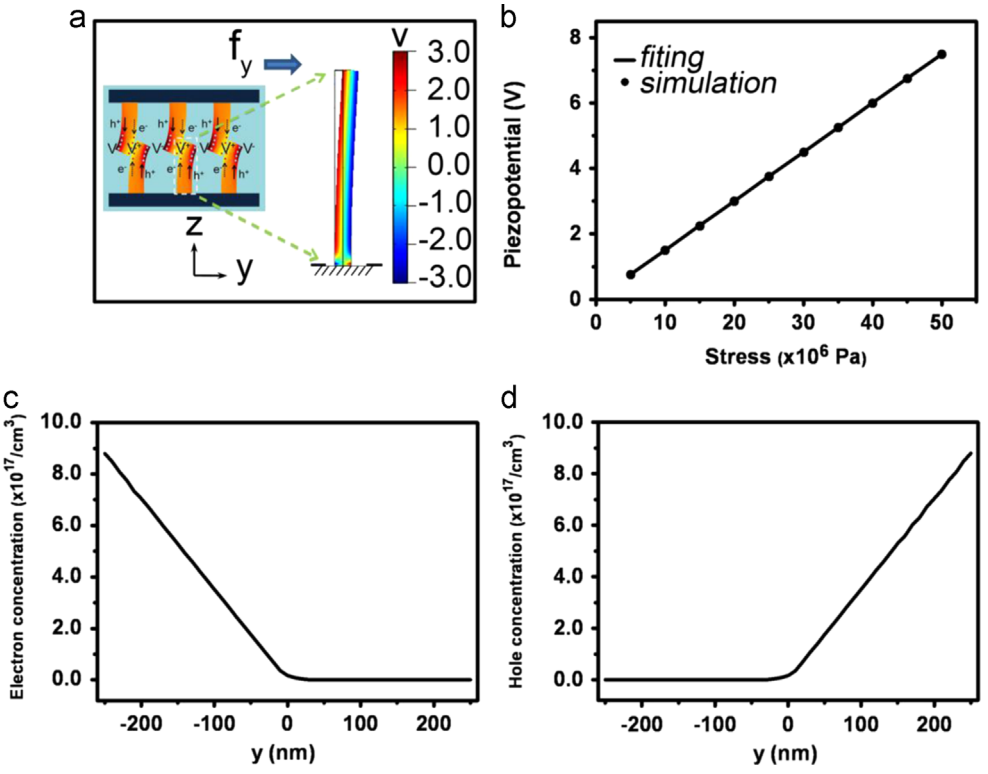

Figure 6 (a) The piezoelectric potential distribution of ZnO nanowire; (b) piezo-potential with applied stress; (c, d) electron and hole concentration distribution with piezo-potential inside ZnO nanowire.

solar and mechanical energy in the nature for water pollution degradation in the future environmental remediation.

Experimental section

ZnO nanowire arrays were synthesized on CFs by a simple seed-assisted hydrothermal method. First, CFs with the length of 10 cm were washed with alcohol and deionized water for several times to remove surface impurities. Zn $(CH_3COO_2)_2 \cdot H_2O$ solution (10 mM in ethanol) was dropped onto the pre-cleaned CFs and blown dry with nitrogen gas (this process was repeated for several times). The samples were annealed at 350 °C for 20 min in argon ambience to yield a thin layer of ZnO seeds on CFs. Then the seed-modified CFs (ultrasonically cleaned with acetone, deionized water and alcohol, respectively, and dried at 60 °C in air) were immersed into 50 mL water containing 0.596 g Zn $(NO_3)_2 \cdot 6H_2O$ and 0.280 g hexamethylenetetramine (HMTA). After the solution being kept at 90 °C for 4 h, the CFs coated with ZnO nanowire arrays were taken out of the solution, washed with deionized water and alcohol, and dried at 70 °C in air. The products were then annealed at 400 °C for 4 h in argon ambience so that ZnO nanowires were firmly covered on CFs avoiding the nanowires scratching/stripping off during mechanical pulling/releasing. Finally, several bundles of ZnO nanowires/CFs were woven together with multi-fiber structures for the piezo-photocatalytic measurements. The weight ratio of ZnO nanowires: CFs is about 1:1 by weighing CFs before and after coating with ZnO nanowires.

The crystal phases of the obtained ZnO nanowires/CFs were characterized by X-ray diffraction (XRD, D/max 2550 V, CuKα Radiation). Their morphologies and microstructures were investigated by a scanning electron microscope (SEM, JEOL JSM-6700 F) and transmission electron microscope (TEM, JEOL JEM-2010).

The degradation of MB by the piezo-photocatalytic activity of ZnO nanowires/CFs was performed in an aqueous solution under UV irradiation and periodically applied force. A high-pressure mercury lamp (50 W) with main emission wavelength of 313 nm was used as UV source. 200 mg woven ZnO nanowires/CFs was suspended in 100 mL aqueous solution of MB with a concentration of C_0=5 mg/L. Prior to UV irradiation, the suspension was stirred for 20 min in the dark to ensure the establishment of absorption/desorption equilibrium. During piezo-photocatalytic process, the suspension was slightly stirred and any temperature rise was avoided by ventilation with an electric fan. At the same time, a periodic force was applied on the woven ZnO nanowires/CFs to deform the ZnO nanowires by a stepper motor. 3 mL of sample solution was taken out every 30 min and analyzed by a UV-vis spectrometer (Hitachi U-3010). The dye concentration was measured at $\lambda = \sim 660$ nm, which is the maximum absorption peak of MB. The percentage of degradation is designated as C/C_0 (C is test concentration).

Acknowledgments

This work was partly supported by the Beijing Institute of Nanoenergy and Nanosystems, the Knowledge Innovation Program of the, Chinese Academy of Sciences China (Grant no. KJCX2-YW-M13), the National Natural Science Foundation of China, China (51102041 and 11104025), the Fundamental Research Funds for the Central Universities (N120205001, N120405010), and the Natural Science Foundation of Gansu Province, China (Grant no. 145RJZA226).

Appendix A. Supporting information

Supplementary data associated with this article can be found in the online version at http://dx.doi.org/10.1016/j.nanoen.2015.02.029.

References

[1] A.L. Linsebigler, G.Q. Lu, J.T. Yates, Chem. Rev. 95 (1995) 735–758.
[2] M.R. Hoffmann, S.T. Martin, W.Y. Choi, D.W. Bahnemann, Chem. Rev. 95 (1995) 69–96.
[3] X. Chen, X. Wang, X. Fu, Energy Environ. Sci. 2 (2009) 872–877.
[4] H. Zhou, Y. Qu, T. Zeid, X. Duan, Energy Environ. Sci. 5 (2012) 6732–6743.
[5] J. Zhang, J. Sun, K. Maeda, K. Domen, P. Liu, M. Antonietti, X. Fu, X. Wang, Energy Environ. Sci. 4 (2011) 675–678.
[6] Y. Zheng, J. Liu, J. Liang, M. Jaroniec, S.Z. Qiao, Energy Environ. Sci. 5 (2012) 6717–6731.
[7] N. Shi, X. Li, T. Fan, H. Zhou, J. Ding, D. Zhang, H. Zhu, Energy Environ. Sci. 4 (2011) 172–180.
[8] P. Xu, T. Xu, J. Lu, S. Gao, N.S. Hosmane, B. Huang, Y. Dai, Y. Wang, Energy Environ. Sci. 3 (2010) 1128–1134.
[9] J. Yu, J. Ran, Energy Environ. Sci. 4 (2011) 1364–1371.
[10] J. Sun, G. Chen, Y. Li, R. Jin, Q. Wang, J. Pei, Energy Environ. Sci. 4 (2011) 4052–4060.
[11] Y. Yang, W. Guo, J.J. Qi, J. Zhao, Y. Zhang, Appl. Phys. Lett. 97 (2010) 223113.
[12] H.B. Zeng, W.P. Cai, P.S. Liu, X.X. Xu, H.J. Zhou, C. Klingshirn, H. Kalt, Acs Nano 2 (2008) 1661–1670.
[13] J.M. Wu, C.-W. Fang, L.-T. Lee, H.-H. Yeh, Y.-H. Lin, P.-H. Yeh, L.-N. Tsai, L.-J. Lin, J. Electrochem. Soc. 158 (2011) K6–K10.
[14] J.M. Wu, Y.-R. Chen, J. Phys. Chem. C 115 (2011) 2235–2243.
[15] S.R. Lingampalli, U.K. Gautam, C.N.R. Rao, Energy Environ. Sci. 6 (2013) 3589–3594.
[16] Y. Wang, R. Shi, J. Lin, Y. Zhu, Energy Environ. Sci. 4 (2011) 2922–2929.
[17] H. Liu, Y. Su, Z. Chen, Z.T. Jin, Y. Wang, J. Hazard. Mater. 266 (2014) 75–83.
[18] I.V. Lightcap, T.H. Kosel, P.V. Kamat, Nano Lett. 10 (2010) 577–583.
[19] J. Tian, Y.H. Sang, G.W. Yu, H.D. Jiang, X.N. Mu, H. Liu, Adv. Mater. 25 (2013) 5075–5080.
[20] W.J. Zhou, G.J. Du, P.G. Hu, G.H. Li, D.Z. Wang, H. Liu, J.Y. Wang, R.I. Boughton, D. Liu, H.D. Jiang, J. Mater. Chem. 21 (2011) 7937–7945.
[21] Y.J. Su, Y. Yang, H.L. Zhang, Y.N. Xie, Z.M. Wu, Y.D. Jiang, N. Fukata, Y. Bando, Z.L. Wang, Nanotechnology 24 (2013) 295401.
[22] X.D. Wang, J.H. Song, J. Liu, Z.L. Wang, Science 316 (2007) 102–105.
[23] Y. Yang, K.C. Pradel, Q.S. Jing, J.M. Wu, F. Zhang, Y.S. Zhou, Y. Zhang, Z.L. Wang, Acs Nano 6 (2012) 6984–6989.
[24] Y.N. Xie, S.H. Wang, L. Lin, Q.S. Jing, Z.H. Lin, S.M. Niu, Z.Y. Wu, Z.L. Wang, Acs Nano 7 (2013) 7119–7125.
[25] S. Bai, L. Zhang, Q. Xu, Y.B. Zheng, Y. Qin, Z.L. Wang, Nano Energy 2 (2013) 749–753.
[26] S. Xu, Y.G. Wei, J. Liu, R.S. Yang, Z.L. Wang, Nano Lett. 8 (2008) 4027–4032.

[27] J.B. Mu, C.L. Shao, Z.C. Guo, Z.Y. Zhang, M.Y. Zhang, P. Zhang, B. Chen, Y.C. Liu, ACS Appl. Mater. Interface 3 (2011) 590–596.
[28] J.Z. Kong, A.D. Li, X.Y. Li, H.F. Zhai, W.Q. Zhang, Y.P. Gong, H. Li, D. Wu, J. Solid State Chem. 183 (2010) 1359–1364.
[29] E.S. Jang, J.-H. Won, S.-J. Hwang, J.-H. Choy, Adv. Mater. 18 (2006) 3309.
[30] M.B. Starr, X.D. Wang, Sci. Rep. 3 (2013) 2160.
[31] Y. Qin, X. Wang, Z.L. Wang, Nature 451 (2008) 809-813.
[32] J.L. Yang, S.J. An, W.I. Park, G.C. Yi, W. Choi, Adv. Mater. 16 (2004) 1661.
[33] U. Ozgur, Y.I. Alivov, C. Liu, A. Teke, M.A. Reshchikov, S. Dogan, V. Avrutin, S.J. Cho, H. Morkoc, J. Appl. Phys. 98 (2005) 041301.
[34] Z.L. Wang, J.H. Song, Science 312 (2006) 242–246.
[35] Y. Gao, Z.L. Wang, Nano Lett. 7 (2007) 2499–2505.
[36] Y. Zhang, Y.F. Hu, S. Xiang, Z.L. Wang, Appl. Phys. Lett. 97 (2010) 033509.
[37] S.M. Sze, Physics of Semiconductor Devices, Wiley, New York, 1981.
[38] Y. Zhang, Y. Liu, Z.L. Wang, Adv. Mater. 23 (2011) 3004–3013.

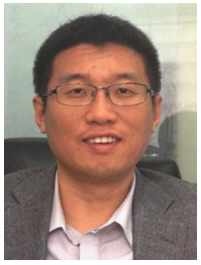

Xinyu Xue is a Professor at College of Sciences, Northeastern University, Shenyang, China. He is also a visiting professor in Beijing Institute of Nanoenergy and Nanosystems, Chinese Academy of Sciences, Beijing, China. Currently he is working on coupling the piezoelectric effect and surface effect.

Weili Zang is currently studying for the master degree in the College of Science, Northeastern University, China. Now her research interests focus on the nanostructured materials for gas sensor and humidity sensor applications.

Ping Deng is currently studying for the master degree in the College of Science, Northeastern University, China. Now her research interests focus on the nanostructured materials for piezoelectric nanogenerators.

Qi Wang is a lecturer at College of Sciences, Northeastern University, Shenyang, China. He mainly focuses on photocatalytic properties of metal oxide nanostructures.

Lili Xing is an Associate Professor at College of Sciences, Northeastern University, Shenyang, China. She mainly focuses on the synthesis of metal oxide nanostructures.

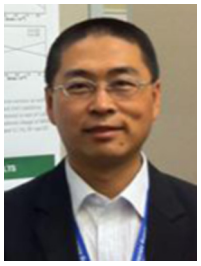

Yan Zhang received his B.S. degree (1995) and Ph.D. degree in Theoretical Physics (2004) from Lanzhou University. Then, he worked as a lecturer, associate Professor (2007), and Professor (2013) of Institute of Theoretical Physics in Lanzhou University. In 2009 he worked as research scientist in the group of Professor Zhong Lin Wang at Georgia Institute of Technology. His main research interest and activities are: self-powered nano/micro-system, theoretical calculation of piezotronic, dynamics of time-delay systems and complex networks.

Zhong Lin Wang received his Ph.D. from Arizona State University in physics. He is now the Hightower Chair in Materials Science and Engineering, Regents' Professor, Engineering Distinguished Professor and Director, Center for Nanostructure Characterization, at Georgia Tech. Dr. Wang has made original and innovative contributions to the synthesis, discovery, characterization and understanding of fundamental physical properties of oxide nanobelts and nanowires, as well as applications of nanowires in energy sciences, electronics, optoelectronics and biological science. His discovery and breakthroughs in developing nanogenerators established the principle and technological roadmap for harvesting mechanical energy from the environment and biological systems for powering a personal electronics. His research on self-powered nanosystems has inspired the worldwide effort in academia and industry for studying energy for micro-nano-systems, which is now a distinct disciplinary in energy research and future sensor networks. He coined and pioneered the field of piezotronics and piezo-phototronics by introducing piezoelectric potential gated charge transport process in fabricating new electronic and optoelectronic devices. Details can be found at: http://www.nanoscience.gatech.edu.